Impact of ASCAT Scatterometer Wind Observations on the High Resolution Limited Area Model (HIRLAM) in an Operational Context

Article *in* Weather and Forecasting · April 2013

DOI: 10.1175/WAF-D-12-00056.1

CITATIONS
8

READS
249

4 authors, including:

Siebren De Haan
Koninklijk Nederlands Meteorologisch Instituut
61 PUBLICATIONS **1,446** CITATIONS

SEE PROFILE

G. J. Marseille
Koninklijk Nederlands Meteorologisch Instituut
80 PUBLICATIONS **577** CITATIONS

SEE PROFILE

Impact of ASCAT Scatterometer Wind Observations on the High Resolution Limited Area Model (HIRLAM) in an Operational Context.

Siebren de Haan, Gert-Jan Marseille, Paul de Valk and John de Vries

Gert-Jan.Marseille@knmi.nl
Wilhelminalaan 10
3732 GK De Bilt
KNMI, The Netherlands

Abstract

Denial experiments, also denoted Observing System Experiments (OSEs), are used to determine the impact of an observing system on the forecast quality of a Numerical Weather Prediction (NWP) model. When the impact is neutral or positive, new observations from this observing system may be admitted to an operational forecasting system based on that NWP model. A drawback of the method applied in most denial experiments is that they neglect the operational time constraint on the delivery of observations. In a ten-week twin experiment with the operational High Resolution Limited Area Model (HIRLAM) at KNMI, the impact of additional ocean surface wind observations from the Advanced Scatterometer (ASCAT) on the forecast quality of the model has been verified under operational conditions. In the experiment, the operational model was used as reference, parallel to an augmented system in which the ASCAT winds were assimilated actively. Objective verification of the forecast with independent wind observations from moored buoys and ASCAT winds revealed a slight improvement in forecast skill as measured by a decrease in observation-minus-forecast standard deviation in the wind components for the short range (up to 24 hours). A subjective analysis in a case study showed a realistic deepening of a low pressure system over the North Atlantic near the coast of Ireland through the assimilation of scatterometer data that was verified with radiosonde observations over Ireland. Based on these results the decision was made to include ASCAT in operations at the next upgrade of the forecasting system.

1. Introduction

In this paper we assess the impact of ocean surface wind observations from the ASCAT scatterometer in the operational KNMI HIRLAM setting (Unden, 2002). HIRLAM is a consortium of European meteorological institutes for cooperative research with the aim to develop and maintain a short-range weather forecasting system for operational use by the participating meteorological institutes. However, the exact implementation of the forecasting system differs between institutes. In the remainder, when we refer to the HIRLAM model, we refer to the implementation at KNMI that is discussed in Section 2.

Many weather centers assimilate scatterometer wind data operationally in their global models since the early 1990's and have demonstrated improved forecast skill (Bi et al., 2010, Hersbach and Janssen, 2007). Some studies were carried out for regional models as well, like ERS-1/2 in HIRLAM (Stoffelen and van Beukering, 1997, Pirkka, 2010) and MM5 (Singh et al., 2008) and also showed positive impacts. An increasing number of institutes use scatterometer wind data operationally in their regional models, yet reporting on impact assessment for NWP in an operational context is limited.

The impact of observing systems in a NWP model is generally determined by denial experiments, i.e., by comparing analyses and forecasts of a control experiment using all observations in the analysis with a similar experiment denying the observation type under investigation. Most of these experiments are performed off-line, not considering the time latency of observations, i.e., the time delay between the observation time and the actual availability of the observation. However, in daily operations, latency in data availability has a direct effect on the performance of regional models with short assimilation windows of typically 1-6 hours. Data latency is therefore taken into account in the experiments discussed in the following sections. For synoptic surface observations the latency is in the order of minutes, while for radiosondes it can be up to one hour from the moment of launching the balloon. The availability of satellite data for assimilation is related to the downlink moment of the data to the ground station. ASCAT is situated on the polar orbiting satellite METOP-A giving global coverage of ocean surface winds (Figa-Saldaña et al., 2002). Only during a satellite overpass data can be downlinked to the a ground station. At the time of our experiments (2010), the only ground station available for METOP-A was at Spitsbergen (Svalbard). The satellite orbit period of about 100 minutes implied that only half of the observations were available within the required 1h 15 min. for use in the HIRLAM model (see Section 2). The so-called level-0 data needs processing which adds to the latency. As a consequence, the limited number of available satellite observations due to data latency reduces the amount of information of the observing system for the operational HIRLAM model and regional models in general. This was recognized and direct data broadcast over several areas has been implemented since spring 2011 with the EUMETSAT Advanced Retransmission Service (EARS)[‡] to enhance the Atlantic Ocean coverage through additional data dumps from ascending/descending passes over several stations covering the HIRLAM area, including Maspalomas, Lannion and Athens. Also, since spring 2011, the data is dumped twice per orbit, at an additional ground station in Antarctica (McMurdo).

In this paper, we demonstrate the impact of assimilating ASCAT winds in the operational KNMI HIRLAM environment of 2010, taking into account the limited availability of observations due to latency for the 2010 situation. The remainder of this paper is organized as follows. First, an overview of the HIRLAM operational environment at KNMI is given in Section 2, including the nesting of the various model domains, the time scheduling of executing the model for the different domains, the use of observations and the assimilation method. This is followed by a description of the ASCAT ocean surface wind product in Section 3. Section 4 discusses the experimental setup and the impact of assimilating ASCAT data is demonstrated through verification of wind forecasts against independent wind data from buoys and ASCAT. Section 5 presents a case study of the actual deepening of a low-pressure system in the model simulation through the addition of ASCAT data. The last section summarizes the conclusions and provides an outlook on future work.

2. KNMI HIRLAM operational environment

The HIRLAM forecasting system employs a limited-area primitive equations forecast model for the time evolution of the atmospheric state and a 3D-Var data assimilation system (Gustafsson et al., 2001, Lindskog et al., 2001) in cycling mode to blend prior information on the state of the atmosphere from the forecast model with available observations to provide the

[‡] http://www.eumetsat.int/Home/Main/Satellites/GroundNetwork/EARSSystem/EARS-ASCAT/index.htm?l=en

initial state for a subsequent short-range forecast. The current version of the operational HIRLAM system at KNMI is 7.2[§].

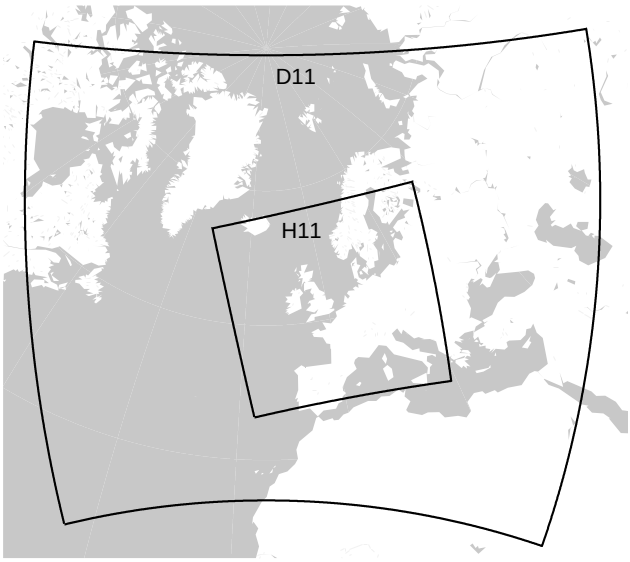

Figure 1. HIRLAM model domains for the D11 (6-hour) and H11 (3-hour) cycles.

The forecasting system operates on two different domains, see Fig. 1, with different cycling schedules, i.e., 4 times per day on the larger domain, in the remainder called the D11 cycle (or D11 run or suite), and 8 times per day on the smaller domain, in the remainder called the H11 cycle (or H11 run or suite). The model equations are identical for both cycles. For both D11 and H11, analyses and forecasts are conducted; for D11 every six hours with a forecast length of 48 hours, and for H11 every three hours with a forecast length of 24 hours. Both cycles have a horizontal grid box size of 11 kilometers. D11 has 60 vertical levels and H11 has 40 vertical levels, both ranging from the surface to the top of the model atmosphere at 0.1 hPa.
Assimilation of observations into NWP models aims at finding the best possible estimate of the atmospheric state, also denoted as analysis, given a short-term forecast, also denoted as first-guess or background, from a previous analysis, new available observations and their respective error characteristics. The analysis serves as forecast initial state from which the forecast is obtained through the integration of the model equations in time and space. Observations used in HIRLAM are discussed below.
For the H11-cycle, a three-hour forecast from the previous H11 run is used as background in the analysis. The D11-cycle uses a six-hour forecast from the previous D11 run as background. Because HIRLAM is a limited area model, the forecast at the domain boundaries is constraint by the model in which it is embedded, i.e., D11 for the H11 run. The D11 run is nested in the global forecast fields from the European Centre for Medium Range Weather Forecasting (ECMWF). H11 and D11 have different observation cut-off times, i.e., the time span between the actual start of the model run, that defines the end of the time window of used observations, and the analysis time. H11 (D11) uses an observation window of 2h30m (5h) with a cut-off time of 1h (2h) respectively. Table 1 summarizes the main characteristics of both runs. As an example, the 12UTC analysis for the H11 run uses the 3-hour forecast from the 09UTC analysis as background. All observations in the time window from 10.30UTC until 13UTC are used in the analysis. The analysis calculation starts at the window

[§] www.hirlam.org

end at 13UTC. Forecasts (FC) are produced from the analyses with a maximum range of 24 hours.

Table 1. Main characteristics of HIRLAM D11 and H11 cycles. Analyses for D11 are obtained for 00, 06, 12 and 18 UTC (t_{an}), i.e., a 6-hour cycle. For H11 analyses are obtained at 03, 09, 15 and 21 UTC in addition, i.e., a 3-hour cycle. The observation time window around the analysis time is obtained from the cycle interval, t_c, and the cut-off time, t_{cut}, through [t_{an} - t_c /2, t_{an} + t_{cut}]. The start of the analysis is at t_{an}+ t_{cut}.

	model grid size (degree)	model levels	cycle interval, t_c, (hours)	cut-off time, t_{cut}, (hour)	lateral boundaries	FC range (hour)
D11	0.1	60	6	2	ECMWF	48
H11	0.1	40	3	1	D11	24

Observations used for the operational run at KNMI are generally obtained through the Global Telecommunication System (GTS) dedicated for the exchange of meteorological observations. Other observation types are also available, such as GPS atmospheric delay, wind and pressure observations from drifting and moored buoys and wind profiler observations, but these are currently not used in the H11 and D11 suites at KNMI. At present the observation set used in the assimilation is composed of aircraft AMDAR (wind and temperature), radiosonde (wind, temperature and humidity) and synoptic stations over land and sea (pressure). Figure 2 shows the typical observation coverage for the 12 UTC analysis time observation window. AMDAR observations are gathered from commercial aircrafts yielding high density wind and temperature observations near airports during ascent and descent. Over the Atlantic Ocean, at cruise level, observations are obtained only at 7 minute intervals corresponding to about 105 km spatial separation. Radiosonde launch sites and Synop stations are generally located over land, with some sparse stations over the ocean. From Fig. 2 it is clear that the oceanic region of the model domain is poorly sampled, in particular for wind and temperature. Satellite data fill this gap.

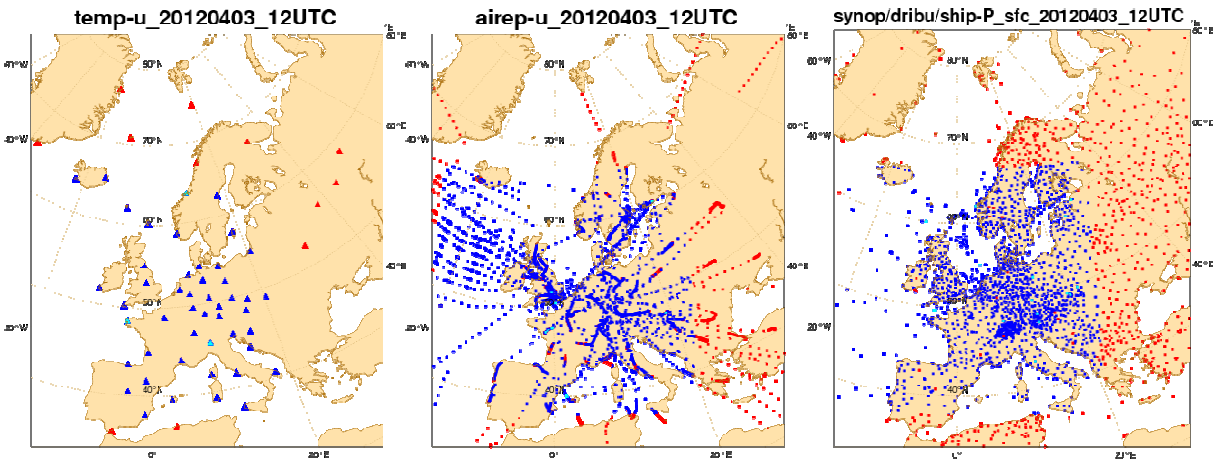

Figure 2. Typical HIRLAM data coverage for the 12 UTC analysis window as obtained from the KNMI experimental observation monitoring tool, including radiosonde profiles (left panel), aircraft (AMDAR) observation (center panel) and surface observations from synop stations, ships and drifting buoys (right panel). Blue (red) symbols denote observations at locations used (not used) in the H11 analysis. Red coloured symbols are either outside the H11 domain as displayed in Figure 1 or flagged as suspect at the quality control stage. Cyan coloured symbols indicate a discrepancy between the observation and corresponding model value, but the corresponding observations were nonetheless used in the analysis.

Observation handling in HIRLAM involves observation screening, reformatting of observation data structures, storage and generating and plotting of observation statistics (e.g. Lindskog et al., 2001). In the screening, logical checks are performed such as a location check for the observations in the model domain. Consistency checks (no SHIP observations over land), blacklisting and white listing to forcefully exclude and include observations from particular stations and/or in particular areas, quality control in the form of a background- or first-guess check to reject observations not consistent with prior information, etc. Additional observation screening is present in the 3D-VAR analysis. Variational quality control (Järvinnen et al., 1997) is built-in to reduce or eliminate the influence of observations inconsistent with the current solution for the analyzed model state in the early stages of the minimization. The 3D-Var assimilation scheme assumes that all observations are valid at analysis time. Observations from Synop stations are available at one hour intervals, but only those observations closest to the analysis time are used in the analysis. Spatial observation thinning is not applied in the operational 3D-Var environment at KNMI.

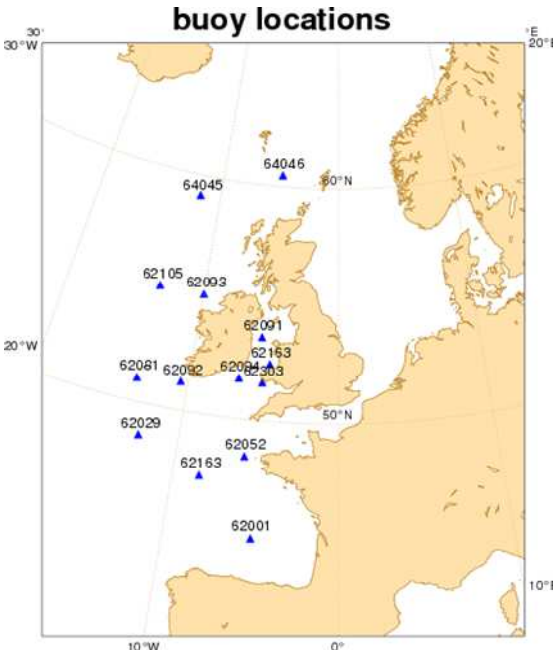

Figure 3. Locations (triangles) and instrument identification numbers of moored buoys.

Pressure and wind observations from drifting and moored buoys are not used in the HIRLAM analysis. Yet, as will be shown later, it was found that wind observations from a selection of moored buoys are of good quality and can be used for the verification of model forecast fields. In general, buoy wind observations are time averaged over 10 minute intervals to reduce observation noise. Moored buoys have also been used for the validation of scatterometer winds (Stoffelen, 1998, Hersbach et al., 2007, Vogelzang et al., 2011). Figure 3 shows the locations of moored buoys whose observations are used for verification in section 4. Table 2 summarizes the usage of the baseline observations in the operational HIRLAM environment.

Table 2: Summary of baseline observations and usage in the HIRLAM analysis, with Y and N denoting Yes and No respectively.

		Parameter	Assimilated
Surface	Synop land	Pressure Wind speed/direction	Y N
	Synop ship/Moored buoys	Pressure Wind speed/direction	Y N
	Drifting buoy	Pressure	N
Upper Air	Radiosonde	Temperature Wind speed/direction Humidity	Y Y Y
	Airep/AMDAR	Temperature Wind speed/direction	Y Y

3. ASCAT scatterometer ocean surface wind observations

The ASCAT scatterometer on board of the low earth polar-orbiting satellite METOP-A is designed to measure the electromagnetic backscatter by the wind-roughened ocean surface (Figa-Saldaña et al., 2002). ASCAT has six antennas, three measuring to the left and three measuring to the right of the satellite track. The system covers two 500 km swaths that are separated from the satellite ground track by about 360 km, see Fig. 4.

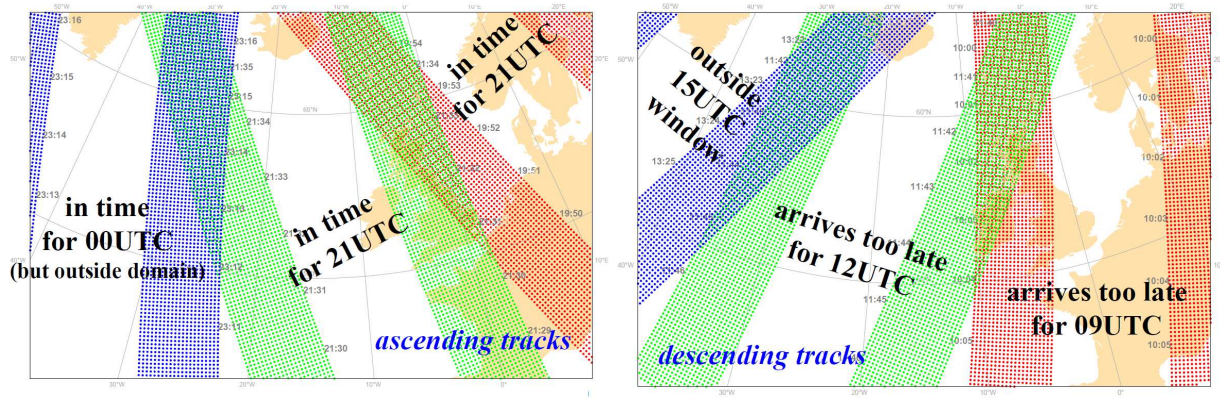

Figure 4. Ascending (left) and descending (right) ASCAT tracks for three different colored overpasses. The overpass time (UTC) is displayed next to the swaths. The dots denote the Wind Vector Cell (WVC) centroids at which the wind observations are defined. Their spatial separation is 25 km. The ASCAT swath has 21 WVCs across track and is 500 km wide. Each panel shows 3 overpasses on 27 April 2010, around 19:51 (rightmost swaths that are in time for the 21 UTC analysis), 21:33 (in time for the 21 UTC analysis) and 23:13 UTC for the left panel (in time for the 00 UTC analysis but outside the HIRLAM H11 domain, see Fig.1) and around 10:03 (observations arrive too late for the 09 UTC analysis), 11:43 (observations arrive too late for the 12 UTC analysis) and 13:24 UTC (observations arrive too late for the 15 UTC analysis) for the right panel, see text for further details.

ASCAT wind information is organised in Wind Vector Cells (WVCs) projected on the instrument swath. The number of WVCs determines the sampling resolution for the surface wind field and the wind information is considered to be independent from one WVC to the next. Each WVC contains between two and four ambiguous wind vector solutions that are the result of the inversion of the CMOD5 wind cone, i.e., the Geophysical Model Function (GMF), for a given set of backscatter values and a given scanning geometry (Stoffelen et al., 1997). Each wind ambiguity is characterised by a solution probability that is determined based on the distance-to-cone residual in the inversion.

The wind ambiguities, solution probabilities and prior information from the ECMWF model 10-m background wind are used in a 2D variational ambiguity removal procedure (Vogelzang et al., 2009) to produce an analyzed surface wind field. This wind field is then used to select the wind vector ambiguity in each WVC tat is closest to the analysis, based on vector difference, as the solution for the observed surface wind. A wind vector solution flag is set to the index of the selected wind ambiguity in each WVC.
Finally, the backscatter measurements, wind ambiguities, scanning geometry and wind vector solution flag among others are made available as an ASCAT wind product (see http://www.knmi.nl/scatterometer) in BUFR and NetCDF format. Current ASCAT products include wind speed and direction information at either 25 km or 12.5 km spacing. The experiments described in this paper use the 25 km product that has an accuracy of 1.3 ms^{-1} in wind speed and 16 degrees in wind direction when compared to collocated ECMWF model winds (Verspeek et al., 2010, Vogelzang et al., 2011).

The orbital period of METOP-A is about 100 minutes. At the time of the experiments full orbit data were down-linked only once per orbit to the Svalbard ground station. On top of the downlink time some additional latency is introduced due to processing of the backscatter signals to ocean surface winds and the dissemination of observations through the GTS. As a consequence, the total time latency for descending orbits is more than 120 minutes, so these data arrive too late for assimilation in HIRLAM. On the other hand, observations from ascending orbits inside the model domain may be assimilated if they fit within the observation window.
Given the above constraints, the HIRLAM observation cut-off time of 1 hour, see Table 1, and the H11 model domain, see Fig. 1, effectively about half the total number of ASCAT observations in the model domain can be used in the analysis, see Fig. 5. Figure 4 shows a typical example with 3 overpasses from the ascending orbit node in left panel. Data from the first overpass (two rightmost swaths) around 19:51 UTC and the seconds overpass around 21:33 UTC are in time for the 21UTC analysis with observation window [19:30, 22:00]. The left most overpass at 23:13 UTC is outside the HIRLAM H11 domain, so the data can not be used for the 00 UTC analysis. Data from the descending orbit nodes in the right panel are downlinked to Svalbard about 1.5 hour after observation time and therefore arrive too late for the analysis.

The HIRLAM implementation for ASCAT winds is to assimilate the components of the wind vector ambiguities. Before ASCAT observations are admitted to the analysis, they first have to undergo a screening procedure. The screening of ASCAT observations consists of a location check for each WVC against the HIRLAM domain and a check on the observation time for each across-track row of WVCs against the observation time window of a given assimilation cycle. In addition a threshold check is performed for the presence of sea ice and land. Finally, the WVC quality flag from the ASCAT wind product is used to ensure the use of winds based on high-quality and complete backscatter measurements and a successful inversion. Because the ASCAT wind information consists of wind ambiguities, no first-guess check is carried out and in the analysis; variational quality control is not active for ASCAT data.

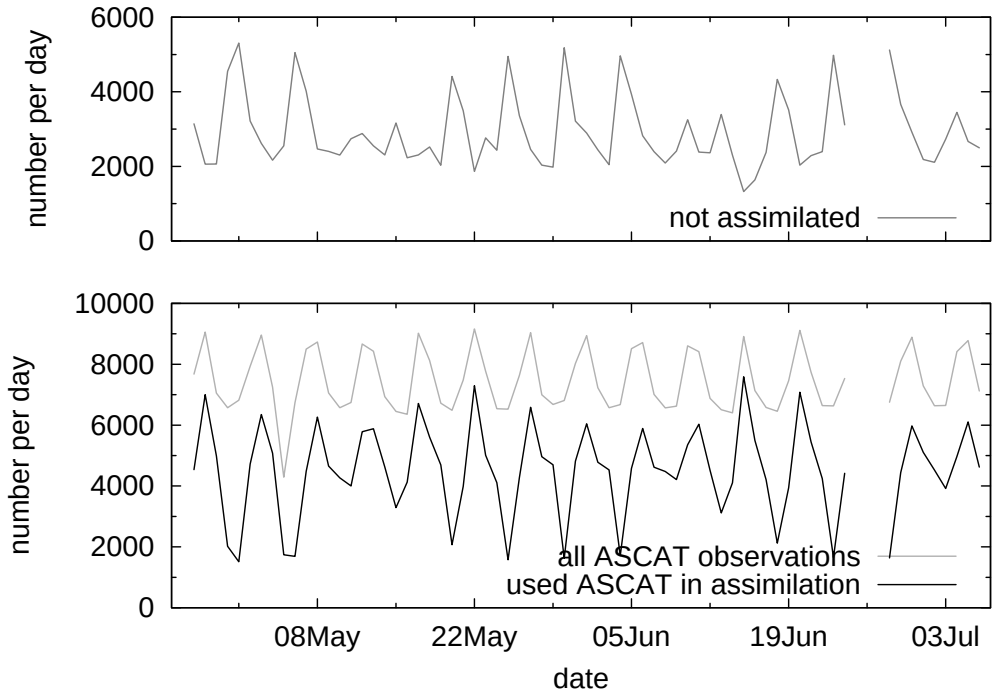

Figure 5. ASCAT observation usage in HIRLAM. Bottom panel: total number of available (gray) and used for assimilation (black) ASCAT observations in the H11 domain, depicted in Fig. 1, per day for the period 24 April until 7 July 2010. The top panel curve shows the difference of the gray and black curves of the bottom panel corresponding to the number of non-used ASCAT observations. The missing part of the curves near 26 June is due to an interruption in operations because of a system upgrade.

In 3D-VAR the cost function

$$J = J_b + J_o \tag{1}$$

is minimized. The component terms in (1) are quadratic forms expressing the 'distance' between the analysis state and the prior or background state and observations respectively. The cost function J_o comprises the contribution of individual observation types, i.e.,

$$J_o = J_{o,SYNOP} + J_{o,ASCAT} + \cdots \tag{2}$$

For ASCAT the cost function is defined as

$$J_{o,ASCAT} = \sum_{j}^{N_{obs}} \left(\sum_{i=1}^{N_j} J_i^{-p} \right)^{-1/p} \tag{3}$$

where

$$J_i = \left(\frac{u - u_i}{\sigma_{o,ASCAT}} \right)^2 + \left(\frac{v - v_i}{\sigma_{o,ASCAT}} \right)^2 - 2 \ln P_i \tag{4}$$

is the cost of the *i*-th ambiguity. N_j is the number of ambiguities in observation j, (u,v) and (u_i, v_i) are the analysis and ASCAT wind vector ambiguity components respectively, $\sigma_{o,ASCAT}$ is the expected standard deviation of the error in the ASCAT wind components with a value of 1.8 ms^{-1} (Vogelzang et al., 2009), P_i is the a-priori solution probability (Portabella and Stoffelen, 2004) and p is an empirical weight factor for the ambiguities which currently has the value of four. This weight factor emphasizes the discrimination between the ambiguities and makes the expression for the cost function behave more as an 'if'-statement.

4. Experimental setup and results

In this section we demonstrate the added value of ASCAT winds for the operational KNMI HIRLAM cycle. Hereto, we conducted an experimental model run (in the remainder denoted X11) parallel in time to the operational H11 run for the 10-week period of 24 April - 7 July 2010, with the only difference the additional use of ASCAT winds in the experimental run. The model domain for H11 and X11 is identical and the boundaries for both H11 and X11 are obtained from D11. The observation cut-off time of one hour, see Table 1, and the used model domain, see Fig. 1, imply that only about half of the ASCAT data in the model domain can be used as discussed in the previous section. As an example, Fig. 6 shows the ASCAT observations used in the 21 UTC experimental (X11) HIRLAM analysis of 27 April 2010. The assimilated swaths correspond to the first two (in time) overpasses in the left panel of Fig. 4.

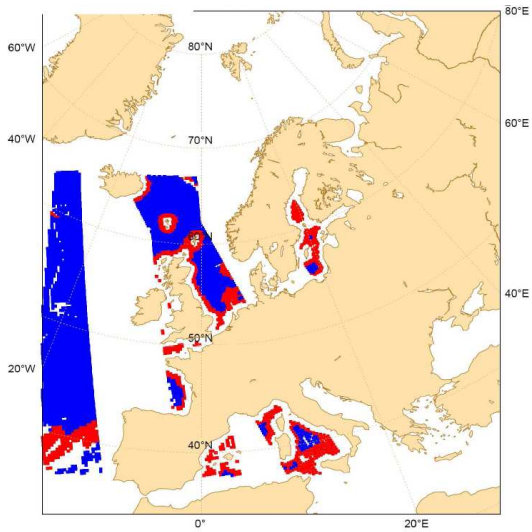

Figure 6. ASCAT observations used in the experimental HIRLAM suite (X11) for the 21 UTC analysis on 27 April 2010. Blue dots denote locations where observations were used in the analysis, red dots denote locations not used in the analysis because of wind retrievals that did not pass the quality control, because of proximity to land, unusual sea state or other surface wind flow regimes not well modelled during the scatterometer wind retrieval, e.g. Stoffelen et al., 1997.

The impact of ASCAT is assessed by comparing the model forecasts from both experiments with independent observations. In an operational context it is also important to monitor the production chain and timeliness of model output for customer delivery, since adding observations to the assimilation will increase the computation time. The parallel set up of the ASCAT experiment guarantees a realistic assessment of the impact obtained from ASCAT observations in an operational environment.

The assimilation experiment was performed in a semi operational environment. Both runs were started almost simultaneously, using exactly the same boundary conditions and baseline set of observations. The parallel run was performed from 24 April to 7 July, 2010. Short interruptions did not cause a break in the assimilation chain of the X11 run through restarts in off-line mode to catch up with the operational model. The restarts were initiated with the latest X11 analysis and identical boundaries and conventional observations as in the operational H11 run plus ASCAT.

The operational ASCAT 25 km product was used in the experiments. The specified observation error for both wind components, that determines the weight of the observations in the analysis, is 1.8 ms^{-1}, similar as used at ECMWF. It is well known that global models lack variance on scales below 200 km (Vogelzang et al., 2011). As a consequence, the

representativeness error of closely spaced observations (separated by less than 200 km) is correlated. However, nowadays assimilation system assume uncorrelated observations. To account for this inconsistency NWP centers apply data thinning and/or inflate the observation error variances to reduce the weight of the observations in the analysis. ECMWF thins ASCAT data to 100 km observation separation. No data thinning and error inflation were applied in the HIRLAM X11 experiment, thus giving substantially more weight to ASCAT observation in the analysis than is done by ECMWF. It should be noted that the forecast range of interest differs for both models with ECMWF focusing in the mid-term (5-10 days) and HIRLAM X11/H11 focusing on the short-range (0-24 hour). This might and most probably will lead to a different use of observations in global and meso-scale models, as further discussed in Section 5.

Results of the assimilation of scatterometer observations is discussed in the following subsection by comparing forecasts of wind and pressure from the H11 and X11 experiments with available independent observations from buoys, ships and ASCAT. We focus on wind and pressure forecasts over the ocean, where maximum impact is expected. The last part of this section describes a case study.

4.1 Objective verification

Forecasts have been compared to independent scatterometer winds for the whole experimental period. Fig. 7 shows a more than 3% reduction of the 10-meter wind speed error standard deviation for the X11 experiment, including ASCAT winds, relative to the operational H11 experiment at FC+06 that gradually decreases to close to neutral at FC+24. The boundary conditions are equal in both H11 and X11 experiments, so the forecasts from both experiments will be nearly identical near the boundaries. Therefore, only scatterometer observations sufficiently remote from the domain boundaries have been used for a valid comparison. Most impact of additional observations is expected in the first couple of hours of the forecast, because the analysis increments induced by the additional observations are advected out of the verification area for longer forecast ranges. Figure 7 shows a positive impact from the ASCAT winds assimilation through a reduction of both the 10-meter wind speed bias and standard deviation over the full forecast range.

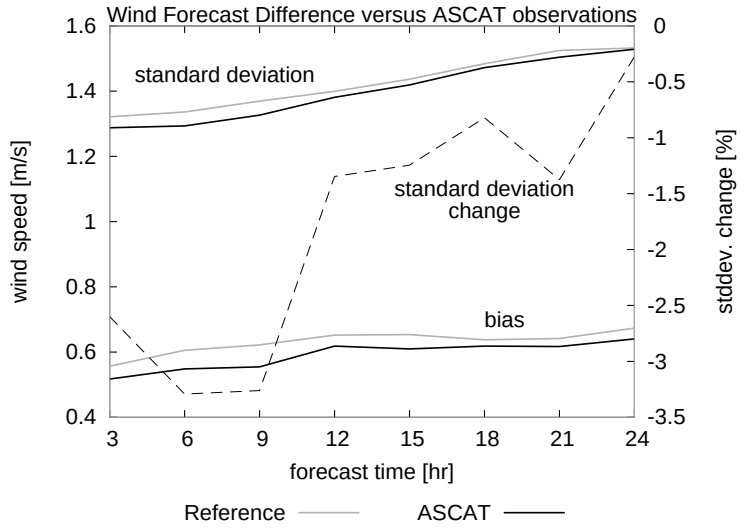

Figure 7. Bias and standard deviation of observation minus forecast (O-F) for 10-meter wind speed from ASCAT and forecasts from the reference H11 run (gray) and experimental (including ASCAT) X11 run (black) for the experimental period 24 April to 7 July 2010. The black dashed line shows the percentage change in standard deviation, with negative values denoting a standard deviation reduction, i.e., improved skill by assimilating ASCAT.

Figure 8 shows the verification of both model suites on 10m winds for the moored buoys displayed in Fig. 3. The wind observations from buoys are currently not assimilated. Yet, the buoy winds are of good quality as can be observed in Fig. 8 from the close to zero bias and standard deviations below 1.8 ms^{-1} for both runs. A positive impact is observed when assimilating ASCAT wind observations. The zonal (east-west) component shows a zero bias for both runs, while the standard deviation is reduced by slightly more than 2% at FC+03 and about 1% at FC+24. For the meridional (north-south) component of the wind, the improvement in standard deviation reduction is even larger from about 2% at FC+03, 3% at FC+12 and slightly more than 1% at FC+24. The meridional wind component shows a small positive bias.

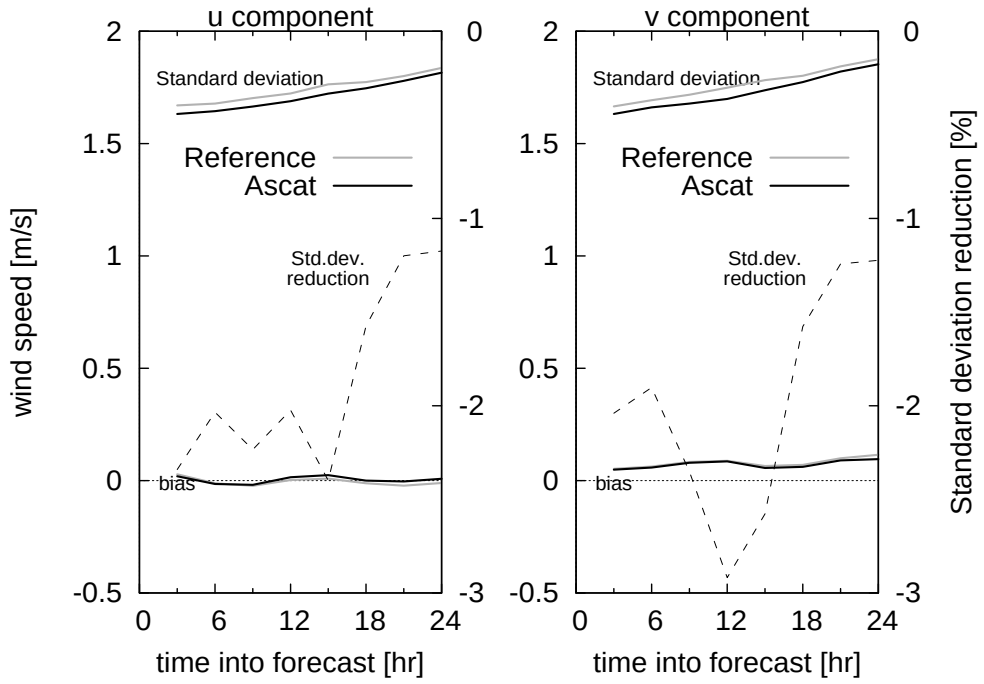

Figure 8. Same as Fig. 7 but now verified against the zonal (u) (left panel) and meridional (v) (right panel) wind components of moored buoys located as displayed in Fig. 3.

Another objective way of verifying observation impact is by evaluating the background departure variances, also denoted observation minus background or (o-b) variances. Background and analysis departures are calculated and archived by default for all observing systems used in HIRLAM. Figure 9 shows that the model winds are consistently closer to buoy measured winds when ASCAT observations are assimilated. This is true for all buoy locations and for both wind components. The (o-b) standard deviation significantly decreases when using ASCAT observations from 1.69 to 1.63 ms^{-1} for the zonal wind component and from 1.69 to 1.62 ms^{-1} for the meridional wind component. Statistical significance was based on the F-distribution[**] with parameters $d_1=d_2=14.535$ and testing the null hypothesis of equal (o-b) variances when using ASCAT data. The F-values for the corresponding 90% and 99% confidence levels then equal 1.027 and 1.044 respectively. The quotient of the (o-b) variances for the zonal and meridional component are 1.075 and 1.088 respectively, i.e., larger than the value for the 99% confidence level, meaning that the null hypothesis should be rejected with more than 99% confidence. The ASCAT impact on the reduction of the (o-b) variance is significant in the sense of the described test above.

[**] http://en.wikipedia.org/wiki/F-distribution

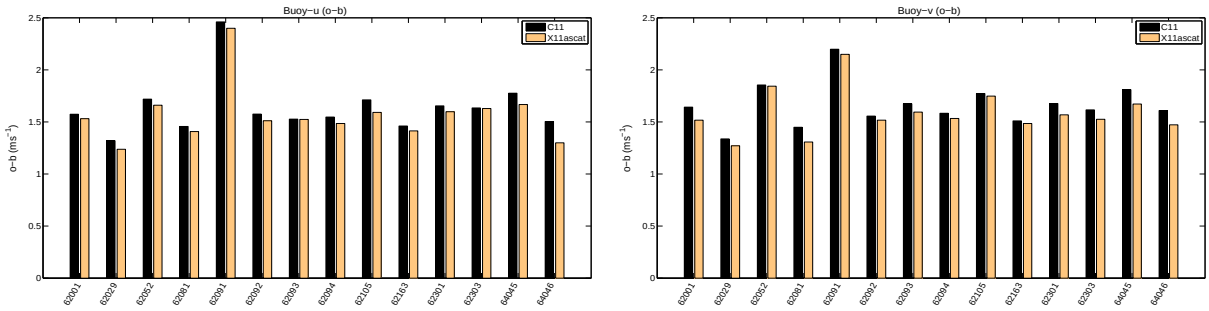

Figure 9. Background departure standard deviation of the HIRLAM model wind from buoy zonal (left panel) and meridional (right panel) wind components, for all buoys separately. The location of the buoys is found in Fig. 3. The statistics are based on 14,535 observations over the complete 10 week experimental period. Black and orange bars correspond to the operational H11 and experimental X11 cycles respectively.

The background departure variance equals by definition the sum of the background error variance and the observation error variance. The latter is composed of the measurement error (instrument noise) variance and the representativeness error variance. For ASCAT observations the standard deviation of (o-b) equals 1.40 and 1.41 ms^{-1} for the zonal and meridional wind components respectively, i.e., smaller than found for buoy winds as expected because buoys yield point observations while ASCAT observations are spatial averages by construction. The representativeness error, which is a substantial component of the background departure, is thus larger for buoys than for ASCAT.

Figure 10 shows the statistics of observation minus forecast for surface pressure from moving ships and the moored buoys (and ships) displayed in Fig. 3. A positive impact is found for positive differences (black lines). Compared to moving platforms, the bias is slightly increased, while the standard deviation is smaller when using ASCAT. For moored platforms, a neutral impact is observed, slightly positive in the first 10 hours of the forecast and slightly negative for larger forecast ranges.

The quality of surface pressure observations from drifting buoys is non-constant for different buoys. Figure 11 shows the standard deviation of the difference of the observed surface pressure and the corresponding HIRLAM reference forecast for a number of buoys. Clearly, the quality differs per buoy. To reduce the impact of quality differences on the results only four buoys, that match best with the HIRLAM model, are used for verification, i.e., numbered 62513, 62504, 62517 and 44622, see the right panel in Fig. 12 for their location. Their location during the experimental period is displayed in the right panel of Fig. 12.

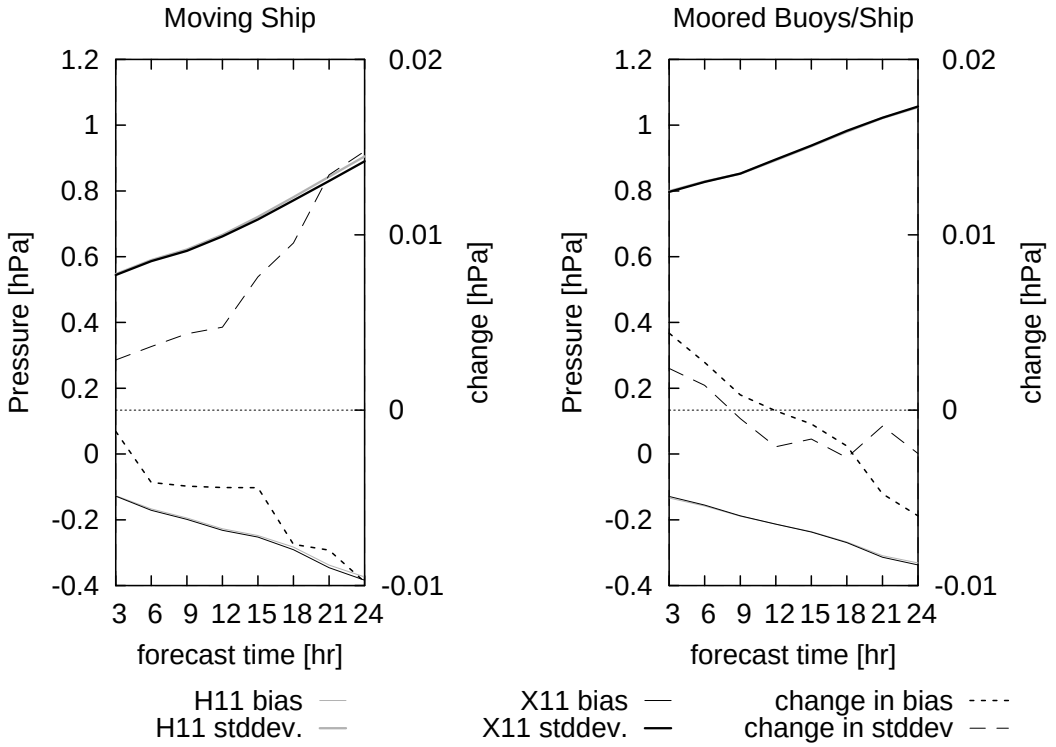

Figure 10. Similar as Fig. 7 but now for pressure observations from moving ships (left) and moored buoys and ships (right). Black dotted lines denote the differences between the absolute bias of the reference (H11) run and the absolute bias of the experimental ASCAT (X11) run. Positive differences imply positive impact.

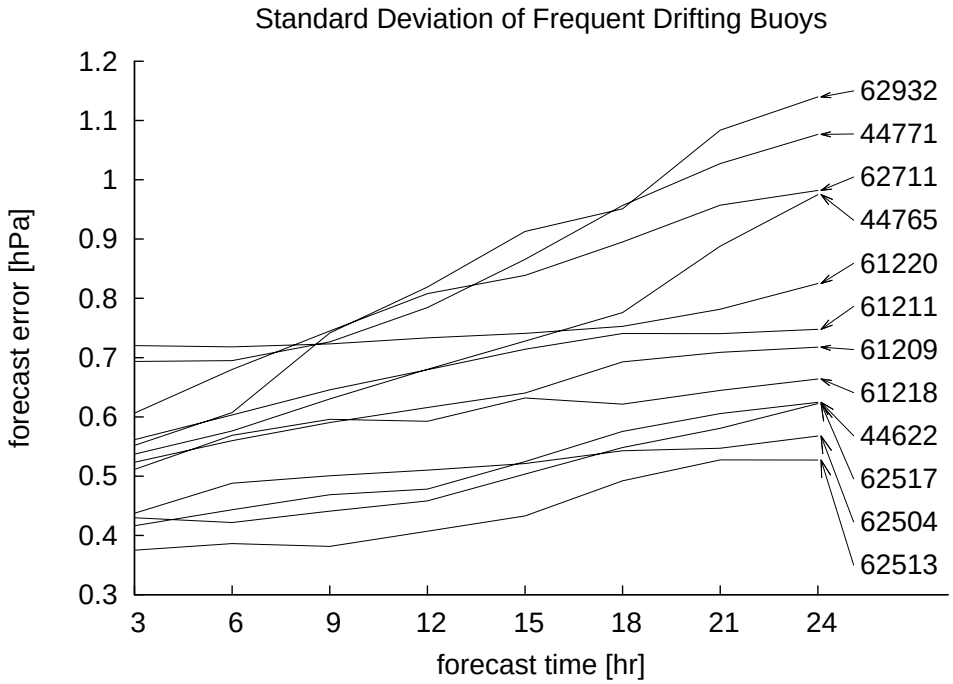

Figure 11. HIRLAM reference model (H11) surface pressure (hPa) error standard deviation against drifting buoys. Some of the buoy locations are displayed in the right panel of Fig. 12.

The pressure observation minus forecast statistics for the selected four drifting buoys is shown in Fig. 12 (left panel). ASCAT data have a small negative impact on the bias and a small positive impact on the standard deviation with forecast time.

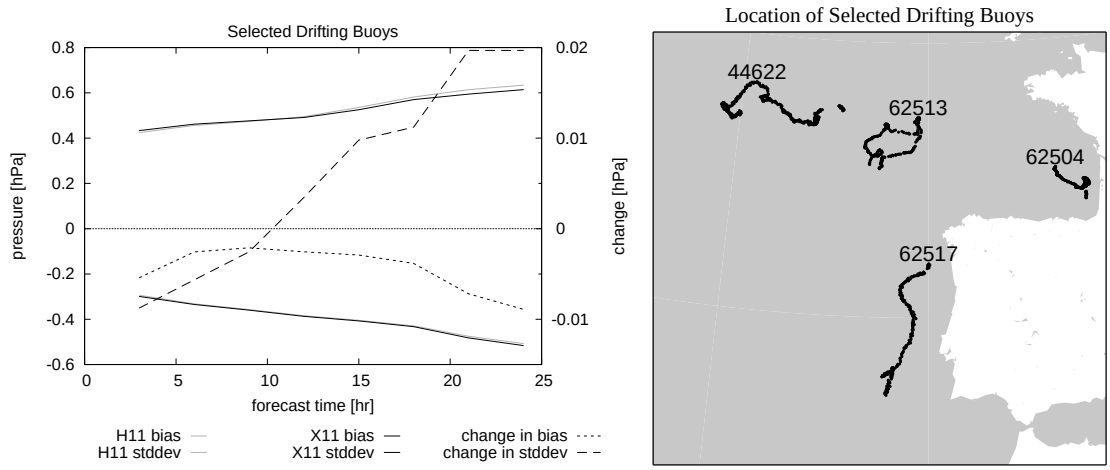

Figure 12. Left panel, same as Fig. 10 but now for the four drifting buoys displayed in the right panel, showing their displacement over the 10 week experimental period.

4.2 Case study: 6 June 2010

On 6 June 2010 around 21 UTC, a low pressure system was situated west of Ireland that moved eastward while slowly filling. On 7 June, the low pressure system reached Ireland around 12 UTC. Figure 13 shows a similar positioning of the low pressure system for both operational H11 and experimental X11, including ASCAT, runs but with small differences in wind speed in the region of high wind speeds south and east of the low pressure system. The lowest value for the mean sea level pressure is 1000 hPa and 997 hPa for the reference and experimental run respectively.

The positioning of the low pressure system at analysis time is close to the HIRLAM domain boundary. The effect of assimilating ASCAT wind is shown by the difference plots of wind speed and mean sea level pressure, depicted in the last column of Fig. 13. The low pressure system is deepened and maintained throughout the complete forecast range. Also, the wind speed increase close to the low pressure system is maintained. The used ASCAT observations are located east of the low pressure system, see Fig. 14. From the analysis increment it is clear that maximum impact of ASCAT observations is obtained near the ASCAT track but the analysis also spatially spreads the observation information to regions outside the swath. Also, regions with plus symbols in the increment indicate an increase of the simulated model wind through the addition of ASCAT observations.

Model wind forecasts from the operational and experimental run were verified against radiosonde data at Valentia (IRL), i.e., 3, 6 and 9-hour forecasts initiated at 6 June 2010 21 UTC and verifying at 7 June 00 UTC, 06 UTC and 12 UTC respectively were compared with successive radiosonde launches at these verification times. Figure 15 shows on average a better match of winds from the experimental (ASCAT) run with the radiosonde winds, in particular for the meridional wind component.
The assimilation of ASCAT wind observations resulted in a slight deepening of the low pressure system, and modestly stronger southerly winds at the Irish coast. Unfortunately, the

deepening of the low pressure system could not be confirmed by pressure observations because of missing moored and drifting buoys near to the location of the low-pressure system.

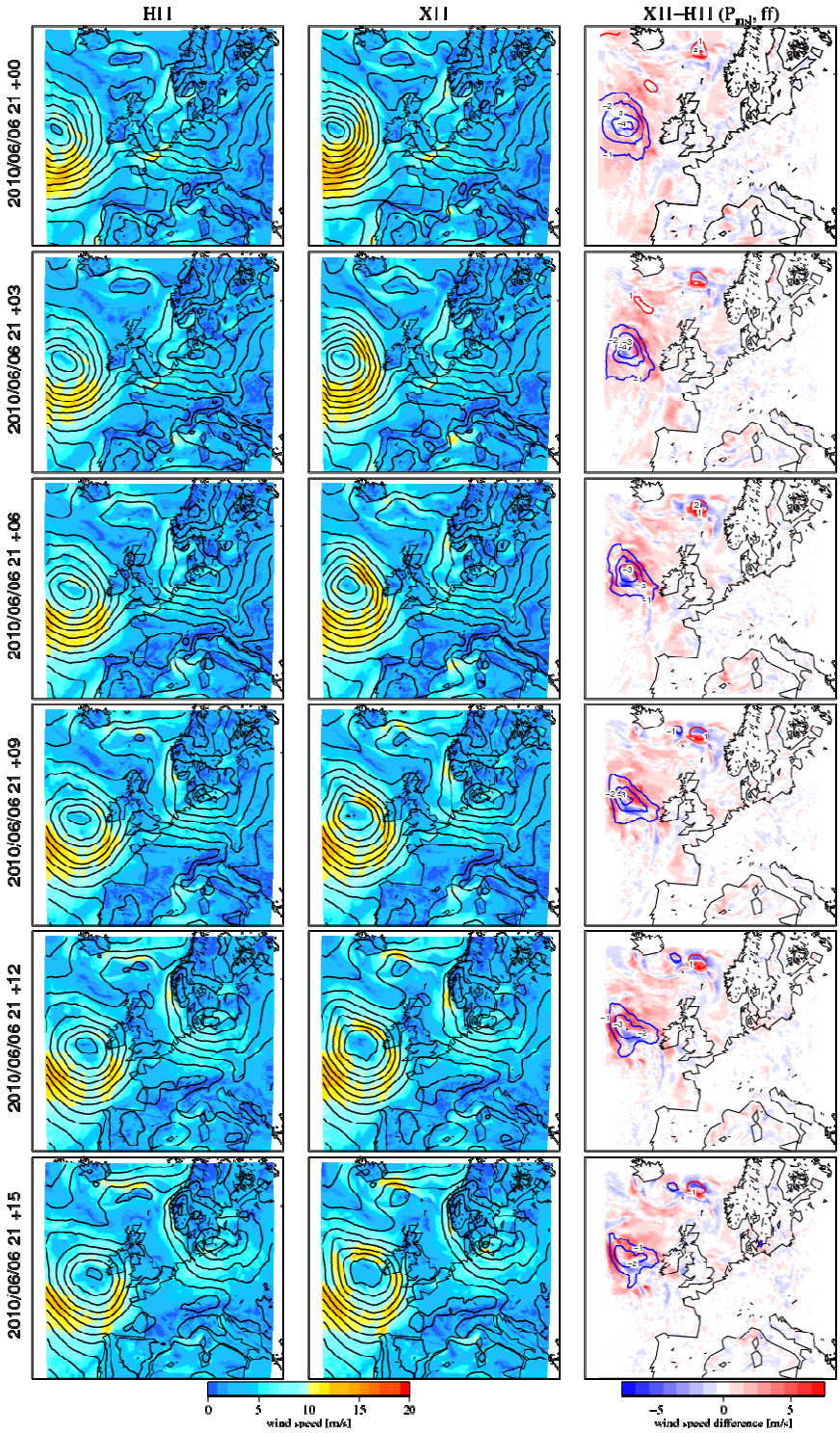

Figure 13: Analyses (top row) and successive forecasts (rows 2-6) of 10-meter wind speed (color scale) and mean sea level pressure (black contours) for the reference (H11) run (first column) and the experimental (X11) ASCAT run (middle column). The last column shows the differences in wind speed (blue to red scale) and mean sea level pressure (blue contours is decrease; red is increase). The analysis time is 6 June 2010 21 UTC. Forecast are shown every 3 hours up to FC+15.

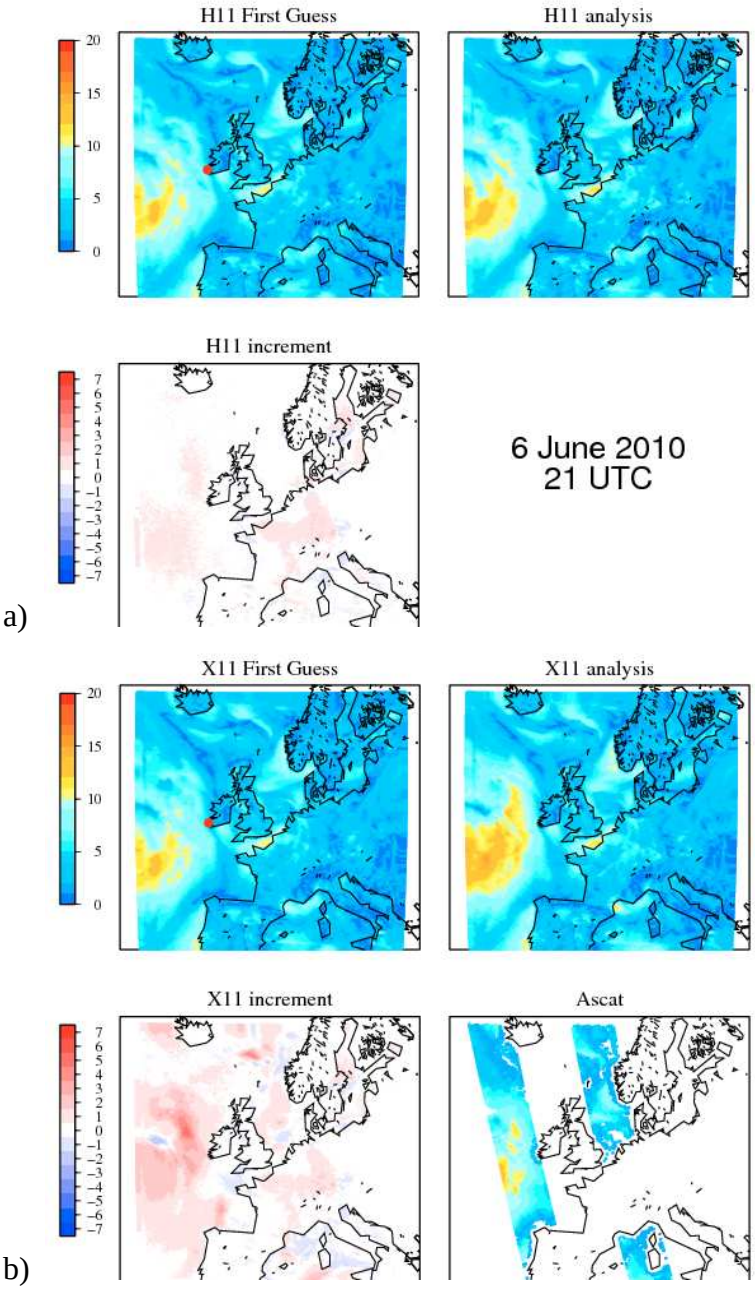

a)

b)

Figure 14. a) 10-meter wind speed background (top left panel), analysis (top right panel) and analysis increment, i.e., analysis minus background (bottom left) for the reference (H11) run. b) Similar but now for the experimental X11 ASCAT run. The bottom right panel shows the ASCAT coverage and measured wind speeds. The red spot in the top left panels marks the location of the observatory in Valentia (Ireland).

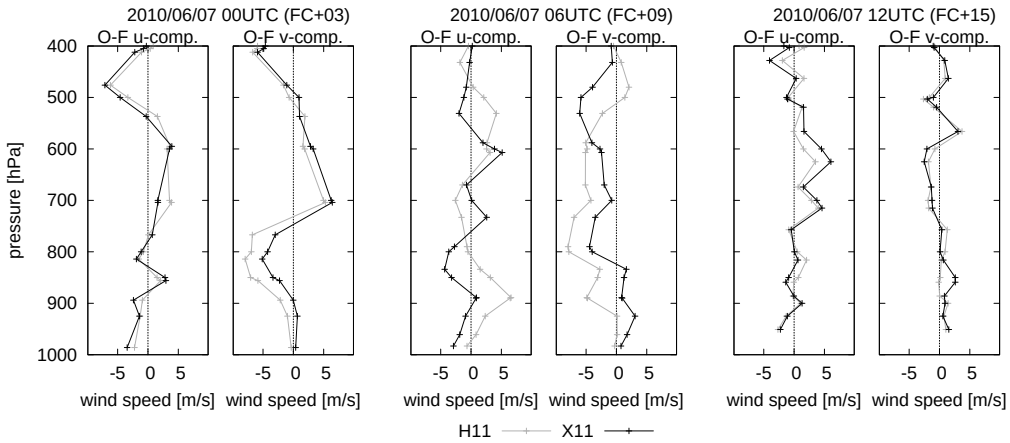

Figure 15: Observation minus forecast for radiosondes launched at Valentia, marked by the circle in Fig. 14. Gray (black) curves correspond to the reference (experimental ASCAT) run. Forecasts are initiated from the 6 June 2010 21 UTC analysis. Left panel: 3-hour forecast minus the 7 June 00 UTC radiosonde launch. Middle panel: 9-hour forecast minus the 7 June 06UTC radiosonde launch. Right panel: 15-hour forecast minus the 7 June 12 UTC radiosonde launch.

5. Summary, conclusions and outlook

ASCAT Scatterometer ocean surface wind observations are proven to be beneficial for the forecast quality of the regional HIRLAM model operational at KNMI. This was demonstrated by comparing the operational cycle with a parallel run over a 10 week period with additional ASCAT wind observations consisting of the ASCAT-25 km data set provided by KNMI in the context of the OSI SAF (Ocean and Sea Ice Satellite Application Facility) project[††]. All other conditions in the operational and parallel run were kept constant, including the conditions at the domain boundaries. Generally, observing system impact experiments do not take into account the operational time constraint on the delivery of observations, which may not be a limitation for most global models, but is an important aspect for regional models with short cut-off times. This paper studied a clean impact experiment taking into account operational conditions at KNMI, including the assimilation window cut-off time and observation delivery through the GTS. Observations arriving too late (later than the window cut-off time) were thus ignored in the analysis. It was shown that at the time that the experiments were conducted in 2010 about half of the ASCAT observations in the model domain could not be used due to these time constraints. Another aspect to consider in an operational context is monitoring of the production chain and timeliness of model output for customer delivery, since adding new observations for assimilation will increase the computation time.

Despite these limitations, wind forecasts verified better against independent (i.e., not assimilated) moored buoys and ASCAT observations with the use of available additional ASCAT data in the analysis. The most substantial improvement was found in the first 12 hours with a 2-3% reduction of the wind components observation-minus-forecast standard deviation decreasing to 1% after 24 hours. The impact on the 24-hour forecast of surface pressure was neutral to slightly positive when compared to ship observations and drifting buoys. A case study showed a realistic deepening of a low pressure system in the North Atlantic near the coast of Ireland through the assimilation of scatterometer data that was verified with radiosonde observations over Ireland.

[††] http://www.osi-saf.org/

The ASCAT experiment was done without additional effort to optimize the information content of ASCAT observations for the HIRLAM model. The observations were used at the highest available density with 25 km spacing between observations. No data thinning or error inflation was applied, which is common practice at most NWP centers. It was found that the ASCAT background departure standard deviation is smaller than the specified 1.8 ms^{-1} observation error standard deviation, meaning that the actual observation error is substantially smaller than specified. The conservative use of observations in the analysis is attributed to the assumption of uncorrelated observation errors. However, nowadays models do not resolve scales below 200 km (Vogelzang et al., 2011), meaning that the representativeness error of closely spaced (less than 200 km separation) observations is correlated. For this reason error inflation is applied to observations with correlated errors to reduce their weight in the analysis. The Hollingsworth and Lönnberg method (Hollingsworth and Lönnberg, 1986) and/or the Desroziers diagnostic method (Desroziers et al., 2005) may be used to separate the observation error and background error from the background departures. In addition, the respective error correlation length scales may be obtained. A better characterization of observation (and model) errors will lead to a more optimal use of observations in NWP models. This will be an active area of research for the coming years thereby keeping in mind the different focal points of global models (medium-range forecast) and meso-scale models (nowcasting, short-range forecast).

Data latency is an important aspect for the *operational* use of observations, in particular for regional models with a more frequent cycling than global models. At KNMI experiments are ongoing with a rapid update cycle of one hour. Latency is not taken into account in standard observing system experiments (OSE) for observation system impact assessment. Standard OSE therefore tend to overestimate the observation impact, in particular when applied to regional models. ASCAT-B observations from the European METOP-B satellite that was launched in September 2012 and expected future access to observations from the Indian and Chinese scatterometers will substantially increase the coverage of ocean surface winds, but their optimal use for regional models will benefit from additional ground stations to deliver the data in time. For ASCAT, and other satellite instruments, the situation has improved substantially through the EARS system. The addition of ground stations since 2011 in the HIRLAM area for fast data delivery of satellite data has reduced the data latency substantially. It is therefore expected that nowadays ASCAT impact on the operational HIRLAM model would be larger than demonstrated in this paper.

Future research activities at KNMI are related to the transition from the hydrostatical HIRLAM model to the non-hydrostatical HARMONIE model. Planned assimilation efforts will focus on the HARMONIE model, including the use of ASCAT, GPS water vapor, high resolution aircraft observations from radar tracking (Mode-S) and radar winds and reflectivity.

Acknowledgement

We thank our colleague Anton Verhoef for the composition of Fig. 4.

References

Bi, L., J. A. Jung, M. C. Morgan, J. F. Le Marshall, 2011: Assessment of Assimilating ASCAT Surface Wind Retrievals in the NCEP Global Data Assimilation System, Mon. Wea. Rev., **139**, 3405–3421. doi: http://dx.doi.org/10.1175/2011MWR3391.1

Desroziers, G., L. Berre,, B. Chapnik, and P. Poli, 2005: Diagnosis of observation, background and analysis-error statistics in observation space, Q.J.R. Meteorol. Soc. 131, pp. 3385-3396.

Figa-Saldaña, J., J. J.W. Wilson, E. Attema, R. Gelsthorpe, M. R. Drinkwater, and A. Stoffelen, 2002: The advanced scatterometer (ASCAT) on the meteorological operational (MetOp) platform: A follow on for the European wind scatterometers, Can. J. Remote Sens., 28(3), 404–412, doi:10.5589/m02-035.

Gustafsson, H., L. Berre, S. Hornquist, X.Y. Huang, M. Lindskog, B. Navascues, K.S. Mogensen and S. Thorsteinsson, 2001:. Three-dimensional variational data assimilation for a limited area model. Part I: General formulation and background constraint. Tellus, 53A, 425-446.

Hersbach, H., and P. Janssen, 2007: Operational assimilation of surface wind data from the MetOp ASCAT scatterometer at ECMWF, ECMWF Newsl., 113, 6–8.

Hersbach, H., A. Stoffelen and S. de Haan, 2007: An improved C-band scatterometer ocean geophysical model function: CMOD5. J. Geophys. Res., 112, C03006, doi:10.1029/2006JC003743

Hoffmann, R. N., 1993: A preliminary study of the impact of the ERS 1 C-band scatterometer wind data on the ECMWF global data assimilation system. J. Geophys. Res., 98(C6), 10233-10244

Hollingsworth, A. and P. Lönnberg, 1986: The statistical structure of short-range forecast errors as determined from radiosonde data. Part 1: the wind field, Tellus, 38A, 111-136

Isaksen, L. and A. Stoffelen, 2000: ERS-Scatterometer Wind Data Impact on ECMWF's Tropical Cyclone Forecasts. IEEE-Transactions on Geoscience and Remote Sensing (special issue on Emerging Scatterometer Applications), Vol. 38 (4), 1885-1892.

Järvinnen, H., P. Unden, 1997: Observation screening and first-guess quality control in the ECMWF 3D-Var data assimilation system. ECMWF Research Department Technical Memorandum No. 236. Available from ECMWF, Shinfield Park, Reading, UK.

Leidner, S. M., L. Isaksen, and R. N. Hoffman, 2003: Impact of NSCAT winds on tropical cyclones in the ECMWF 4D-Var assimilation system, Mon. Weather Rev., 131, 3 –26.

Lindskog, M., N. Gustafsson, B. Navascues, K. S. Mogensen, X. Y. Huang, X. Yang, U. Andrae, L. Berre, S. Thorsteinsson and J. Rantakokko, 2001: Three-dimensional variational data assimilation for a limited area model. Part II.: observation handling and assimilation experiments. Tellus 53A, 447-468.

Marseille, G.J. and A. Stoffelen, 2012: Aeolus Observation Representativeness Error, ESA Technical Note of VHAMP poject, AE-TN-KNMI-VHAMP-007_v1.0

Pirkka, O., 2010: Feasibility of assimilating ASCAT surface winds into a Limited Area Master's thesis , University of Helsinki, Faculty of Science, Department of Physics. https://helda.helsinki.fi/bitstream/handle/10138/20968/feasibil.pdf?

Portabella, M. and A. Stoffelen, 2004: A probabilistic approach for Seawinds data assimilation, Quart. J. Roy. Meteor. Soc., 130, 1-26.

Stoffelen, Ad, and Paul van Beukering, 1997: Improved backscatter processing and impact of tandem ERS winds on HIRLAM, HIRLAM project report nr 31, IMET, Dublin, Ireland.

Stoffelen, A. and D. Anderson, 1997: Scatterometer Data Interpretation: Measurement Space and Inversion, J. Atmos. and Oceanic Technol. 14, 1298-1313

Singh R., P.K. Pal, C.M. Kishtawal and P.C. Joshi, 2008: The impact of variational assimilation of SSM/I and QuikSCAT satellite observations on the numerical simulation of Indian Ocean tropical cyclones. Wea. Forecasting, **23**, 460–476.
doi: http://dx.doi.org/10.1175/2007WAF2007014.1

Stoffelen, A., 1998: Toward the true near-surface wind speed: Error modeling and calibration using triple collocation, . J. Geophys. Res., vol. 103, no. C4, pp. 7755-7766, doi:10.1029/97JC03180

Unden, P., 2002: The HIRLAM version 5.0 model. HIRLAM documentation manual (HIRLAM Scientific Documentation), http://hirlam.org/index.php?option=com_docman&task=doc_details&gid=308&Itemid=139

Verspeek, J.A., A. Stoffelen, M. Portabella, H. Bonekamp, C. Anderson and J. Figa, 2010: Validation and calibration of ASCAT using CMOD5.n, IEEE Transactions on Geoscience and Remote Sensing, vol. 48, 1, 386-395, doi:10.1109/TGRS.2009.2027896.

Vogelzang, J., A. Stoffelen, A. Verhoef, J. de Vries and H. Bonekamp, 2009: Validation of two-dimensional variational ambiguity removal on SeaWinds scatterometer data J. Atm. Oceanic Technol., 7, 26, 1229-1245, doi:10.1175/2008JTECHA1232.1.

Vogelzang, J., Stoffelen, A., Verhoef, A. and Figa-Saldaña, J., 2011: On the quality of high-resolution scatterometer winds, J. Geoph. Res, vol. 116, C10033, 14 pp., doi:10.1029/2010JC006640.